

Effects of Disorder-Induced Symmetry Breaking on the Electroabsorption Properties of a Model Dendrimer

L. Angela Liu, Linda A. Peteanu,^{*,†} and David J. Yaron*

Department of Chemistry, Carnegie Mellon University, 4400 Fifth Avenue, Pittsburgh, Pennsylvania 15213

Received: June 9, 2004

Disorder-induced symmetry breaking is studied in a model dendrimer that consists of three arms arranged with C_3 symmetry. Electroabsorption spectroscopy measurements in the accompanying paper (Bangal, P. R.; Lam, D. M. K.; Peteanu, L. A.; Van der Auweraer, M. *J. Phys. Chem. B* 2004, 108, 16834) show that the dipole moment change of the dendrimer is similar to that of the monomer, suggesting a completely symmetry-broken dendrimer with the excitation localized on one arm of the structure. In this work, we model the symmetry breaking of the dendrimer as a function of its structural disorder. Several collections of disordered dendrimers are created. The excited states of the dendrimer and of the three arms that make up the dendrimer are calculated using the intermediate neglect of differential overlap/singles configuration interaction (INDO/SCI) approach. These data are used to verify and parametrize exciton models that relate the properties of the dendrimer to those of the arms. A binning-and-averaging procedure is introduced so that the calculated electroabsorption properties of the dendrimer can be studied as functions of the energetic disorder in the structure. The excellent agreement between the INDO/SCI method and the exciton models validates the latter models for symmetry-broken structures and demonstrates that diagonal disorder is the dominant form of disorder in the dendrimer. A thorough derivation of the electroabsorption spectrum for C_3 -symmetric molecules indicates that the dipole moment change ratio between the dendrimer and the arm is a sensitive measure of disorder and symmetry breaking. This ratio is $1/\sqrt{2}$ in the absence of disorder, $1/2$ at intermediate disorder, and 1 at large disorder. These results indicate that the experimental dendrimer sample is symmetry-broken.

1. Introduction

Dendrimers may exhibit unusual photophysical and charge-transport properties and have been subject to many experimental and theoretical studies.^{1–10} In this work, we examine a model dendrimer to determine the extent to which its photophysical properties can be understood in terms of the properties of its subunits. We also explicitly connect structural disorder to energetic disorder and study the resulting disorder-induced symmetry breaking.

Dendrimers based on 1,3,5-trisubstituted benzene have been studied as candidate materials for nonlinear optical applications.^{5,11,12} Figure 1b shows a small model dendrimer (*p*-EFTP)^{13–16} of this type. This structure consists of three branches and possesses C_3 symmetry in the absence of disorder. One branch of the dendrimer plus the central benzene ring, *p*-DPABP, is shown in Figure 1a (full names of *p*-EFTP and *p*-DPABP are in ref 17). We refer to the constituent branch structure as the monomer and to the dendrimer as the trimer.

Peteanu's group studied the monomer and the trimer using electroabsorption spectroscopy in a variety of glasses.¹⁷ Electroabsorption spectroscopy measures the change in dipole moment and polarizability of the molecule upon photoexcitation. Their measurements are summarized in Table 1. From these results, Peteanu and co-workers¹⁷ propose that because the trimer and the monomer have similar changes in dipole moment and polarizability, the trimer is symmetry-broken and the excitation of the trimer is localized on one branch.

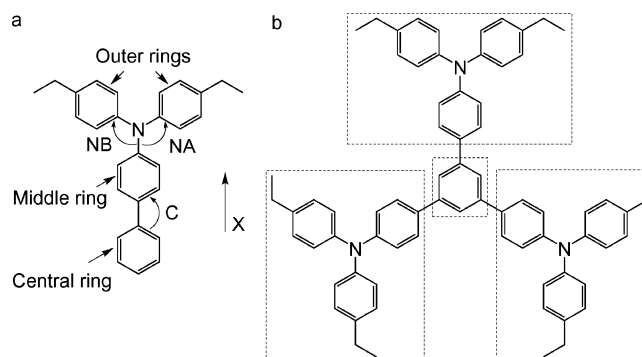


Figure 1. Structures of the monomer *p*-DPABP (a) and the trimer *p*-EFTP (b). The three types of benzene rings are labeled according to their positions in the molecule. C, NA, and NB are the dihedral angles used in building the structures with different degrees of distortion. The rectangles in b represent local segments of the molecule used in calculating the charge-transfer and the excitation localization characters of the excited states (section 2.2). The X axis of the structures is indicated.

TABLE 1: Electroabsorption Spectroscopy Measurements on the Monomer and the Trimer in a Variety of Glasses¹⁷

property	monomer	trimer
dipole moment change (D)	6.0 ± 0.6	6.9 ± 0.6
polarizability change (trace) (\AA^3)	100 ± 30	140 ± 40
maximum absorption (eV)	3.70 ± 0.08	3.54 ± 0.07

The purpose of this work is to model the effects of symmetry breaking induced by geometrical and energetic disorder on the photophysical properties of these systems. We also study the nature of the excitations of these molecules in disordered

* Corresponding author. E-mail: yaron@cmu.edu.

† E-mail: peteanu@andrew.cmu.edu.

samples. Calculations are performed using three methods. First, the intermediate neglect of differential overlap/singles configuration interaction (INDO/SCI) method (section 2.2) is used to study the electroabsorption properties of the monomer and the trimer. Second, a four-state exciton model (section 2.3) is constructed that relates the properties of the trimer to those of the constituent monomers. Third, a simplified exciton model that deals with only diagonal energetic disorder (section 2.4) is built. Such exciton models are commonly used in modeling symmetric dendrimers.^{6,7,12,18} However, relatively few studies have focused on disordered dendritic systems using exciton models. (Off-diagonal disorder was considered in refs 12 and 18.) In this work, the two exciton models cover different subsets of the types of disorder considered in the INDO/SCI methods. Therefore, the comparison between these three methods provides a means to quantify the effects of various types of disorder.

The electroabsorption properties of both the monomer and the trimer are influenced by geometrical distortions in the structures. Therefore, a large number of structures with different degrees of geometrical disorder are needed to capture the structure–function relationships. In this work, we construct several collections of monomer and trimer structures with varying degrees of disorder and study the properties averaged over these collections.

We have found the following from the calculations of these collections of molecules. First, the exciton models that relate the properties of the trimer to those of the arms are verified on the basis of their excellent agreement with the INDO/SCI method. This agreement demonstrates that such exciton models can be used in modeling symmetry breaking in dendrimers. Second, the calculation results confirm that the experimental trimer sample¹⁷ is symmetry-broken, with an energetic disorder among the three arms that is greater than 4 times the interbranch coupling energy. Furthermore, our studies suggest that the experimental monomer sample is more disordered than the trimer sample.

We note here that for C_3 -symmetric molecules the interpretation of the electroabsorption spectrum is complicated by the existence of two degenerate bright excited states with antiparallel dipole moments. For this reason, a detailed derivation of the electroabsorption spectrum (see Supporting Information) is carried out for isotropic C_3 -symmetric molecules, relating the dipole moment change of the trimer to that of the monomer. This derivation together with our collection studies shows that the dipole moment change ratio between the trimer and the monomer is a sensitive measure of symmetry breaking.

2. Methods and Models

2.1. Geometry Optimization. Disorder in the monomer is largely a function of the variability in the three dihedral angles, labeled C, NA, and NB in Figure 1a. C is referred to as the central twist; NA and NB are referred to as the outer twists. Monomers with different twists were obtained through geometry optimization at the AM1^{19,20} level using MOPAC. For each structure, C, NA, and NB were fixed at the specified values, whereas all other coordinates were optimized. In the monomers, the central ring defines the X – Y plane. The X axis, defined in Figure 1, points from the center of the central ring to the nitrogen atom.

The global minimum-energy (heat of formation) structure of the monomer is found to have $C = 40^\circ$ and $NA = NB = 35^\circ$. In this structure, the middle ring and the two outer rings are arranged with C_3 symmetry around the nitrogen, analogous to a propeller.

A collection of 1500 different monomer structures was generated. The dihedral twist C was chosen randomly between 15° and 90° . NA and NB were chosen randomly between 28° and 70° .²¹ The heats of formation of these structures span $\sim 3k_B T$ (about $1.8 \text{ kcal}\cdot\text{mol}^{-1}$ or 600 cm^{-1}) above the minimum-energy structure. Here, k_B is the Boltzmann constant, and T is room temperature. At this value, 95% of a room-temperature thermal distribution is captured.

Because a goal of this work is to relate the properties of the trimer to those of the constituent monomers, we built the trimer by assembling three optimized monomer geometries. We fixed the coordinates of the first monomer and rotated the other two 120° and 240° around the Z axis, respectively. We then superimposed the three structures at their central rings. The central ring of the resulting trimer defines the X – Y plane. The X axis of the first monomer becomes the X axis for the trimer. No further optimization is performed for the trimer. Trimers with three identical arms are C_3 -symmetric. Asymmetric trimers were also built. Different trimers (500) were constructed from the 1500 monomers using 500 sets of three different monomers. These structures are referred to as the 500-trimer collection.

In addition, a smaller collection of ~ 30 trimers was constructed with the special property that the excitation energies of the three monomers, calculated as in section 2.2, are evenly spaced. This property has the advantage of allowing a reliable identification of the three excited states of the trimer that arise from the mixing of the monomer excitations (section 3.2.1). This collection is referred to as the 30-trimer collection.

2.2. INDO/SCI Method. The electronic states are calculated using the INDO/SCI approach. A direct configuration interaction method is used to allow the inclusion of all molecular orbitals in the SCI calculation.²² The dipole moment is obtained as expectation values of the dipole operator. The polarizability is obtained using a finite field method^{23,24} based on the dipole change induced by an external field with a magnitude of $5 \times 10^5 \text{ V}\cdot\text{cm}^{-1}$. This field is comparable to that applied experimentally.¹⁷ Unless otherwise noted, the absolute value of the dipole moment change and the trace of the polarizability change will be reported.

A local orbital method²⁵ was extended to dendritic systems. This method allows us to calculate the excitation localization percentage on each segment of the molecule, defined in Figure 1b, as well as the charge-transfer character between the segments. These properties are used to assign the excited states in the trimer.

In some cases, more than one excited state is predicted to lie in the spectral region of the observed one-photon spectra ($\sim 0.3 \text{ eV}$ in width). Therefore, the spectroscopic properties are averaged using the calculated transition intensities as weights, shown as the following

$$X = \frac{\sum_i^N |\underline{TM}_i|^2 X_i}{\sum_i^N |\underline{TM}_i|^2} \quad (1)$$

where i is the i th excited state and \underline{TM}_i is the i th state transition moment. The underline is used to represent a vector property. X refers to the property being studied (i.e., the excitation energy, the dipole moment change, or the polarizability change). All states that carry significant optical intensity and are within 0.3 eV of the dominant one-photon state are included in the summation of eq 1. This corresponds to one or two states for

the monomer and two or three states for the trimer. The scenarios in which eq 1 can be used will be discussed in detail in section 3.2.3.

2.3. Four-State Exciton Model. We now consider a four-state exciton model that relates the properties of the trimer to those of the constituent monomers. The model uses four basis functions: the ground state $|gs\rangle$ where all three monomers are in their ground state and three excited states $|i\rangle$ ($i = 1, 2, 3$) in which monomer i is excited. The excitation energy, transition moment, and dipole moment change of the i th monomer are denoted E_i^m , TM_i^m , and $\Delta\mu_i^m$, respectively. In this paper, m represents the monomer, and t represents the trimer. Symbols with one and two underlines represent vectors and matrices, respectively. The Hamiltonian of a trimer can be expressed using the excitation energies of the three arms and the coupling energy between the arms as

$$\underline{\underline{H}}^t = \begin{pmatrix} 0 & 0 & 0 & 0 \\ 0 & E_1^m & J & J \\ 0 & J & E_2^m & J \\ 0 & J & J & E_3^m \end{pmatrix} \quad (2)$$

where J is the coupling energy between the branches. The dipole operator of the trimer can be expressed using the transition moments and the dipole moment changes of the three arms as

$$\underline{\underline{\mu}}^t - \langle gs | \underline{\underline{\mu}}^t | gs \rangle = \begin{pmatrix} 0 & \underline{TM}_1^m & \underline{R TM}_2^m & \underline{R^2 TM}_3^m \\ \underline{TM}_1^m & \underline{\Delta\mu}_1^m & 0 & 0 \\ \underline{R TM}_2^m & 0 & \underline{R \Delta\mu}_2^m & 0 \\ \underline{R^2 TM}_3^m & 0 & 0 & \underline{R^2 \Delta\mu}_3^m \end{pmatrix} \quad (3)$$

where \underline{R} corresponds to a rotation about the Z axis by 120° . Each matrix element in eq 3 is a vector property in 3-D space. The excited states of the trimer are obtained by diagonalizing the Hamiltonian and transforming the dipole operator.

Disorder and symmetry breaking are included in the model by allowing the excitation energies, the transition moments, and the dipole moment changes in eqs 2 and 3 to be different. If the excitation energies are different, such disorder is called diagonal disorder. If the coupling energy J is different among the different branch pairs, then such disorder is called off-diagonal disorder. When the transition moments and the dipole moment changes are different, such disorder is called dipole operator disorder.

Below, we investigate the validity of this four-state exciton model by comparing its predictions to those of explicit INDO/SCI calculations for the 500-trimer collection of section 2.1. The properties E^m , TM^m , and $\Delta\mu^m$ in eqs 2 and 3 are obtained from INDO/SCI calculations on the monomers. If the model agrees with the INDO/SCI calculations, then the properties of the trimer are indeed related to those of the monomer via a four-state exciton model.

In this exciton model, the interbranch coupling energy J is parametrized by minimizing the relative errors between the results obtained from the four-state exciton model and those from the INDO/SCI method for the 500-trimer collection. On the basis of a least-squares analysis of the excited-state energies and dipole moment changes, J is found to be ~ 0.05 eV. All results of the four-state exciton model presented in this article were obtained with $J = 0.05$ eV. Because a single value is used for the coupling term, off-diagonal disorder is ignored in this

TABLE 2: Types of Disorder Considered in Each Method in the Study of the Trimer

disorder type	INDO/SCI method	four-state exciton model	diagonal disorder exciton model
diagonal	✓	✓	✓
off-diagonal	✓	×	×
dipole operator	✓	✓	×

model. Therefore, the differences between this model and the INDO/SCI method provide insights into the importance of off-diagonal disorder. Harigaya¹² and Martín-Delgado et al.¹⁸ have considered only off-diagonal disorder in their study of dendrimers. It should be noted that their dendrimers have very large interbranch coupling energies on the order of 1 eV, making off-diagonal disorder dominant.

2.4. Diagonal Disorder Exciton Model. A simpler exciton model can be constructed considering only the diagonal disorder. The Hamiltonian of this model takes the following form

$$\underline{\underline{H}}^t = \begin{pmatrix} 0 & 0 & 0 & 0 \\ 0 & E^m + r_1 & J & J \\ 0 & J & E^m + r_2 & J \\ 0 & J & J & E^m + r_3 \end{pmatrix} \quad (4)$$

where E^m is the experimental maximum absorption energy or λ_{\max} of the monomer and r_i ($i = 1, 2, 3$) is a random number centered at zero and distributed with a standard deviation of $|r|$. If we assume the absorption curve has a Gaussian shape, then the full width at half-maximum (fwhm) of the monomer absorption peak, or the inhomogeneous line width, is $2.355|r|$. Thus, the exciton model includes diagonal disorder that corresponds to an experimental observable. For each value of $|r|$, a million matrices are generated so that the reported averages are well converged.

Equation 4 assumes that disorder primarily alters the energy of the monomers. The coupling between the arms, J , and the dipole operator are assumed to be constants that are independent of structural disorder. A comparison of this diagonal disorder model with the four-state exciton model and the INDO/SCI method provides insight into the effects of diagonal disorder and dipole operator disorder on the trimer's properties.

The parameters used in this model are monomer excitation energy $E^m = 3.7$ eV, monomer transition moment $|TM^m| = 7$ D, monomer dipole moment change $|\Delta\mu^m| = 4.5$ D, and interbranch coupling energy $J = 0.05$ eV.

Table 2 summarizes the various types of disorder that are captured by the above three methods: the INDO/SCI method (section 2.2), the four-state exciton model (section 2.3), and the diagonal disorder exciton model (section 2.4). A comparison of these three methods reveals the importance of each type of disorder in the symmetry breaking of the trimer.

3. Results

3.1. Properties of the Monomer. The INDO/SCI calculation on the minimum-energy structure of the monomer (section 2.1, $C = 40^\circ$ and $NA = NB = 35^\circ$) yields the following: the excitation energy is 3.57 eV, the dipole moment change is 5.5 D, the transition moment is 6.5 D, and the polarizability change is 175 \AA^3 . These properties of the monomer are sensitive to the geometry. As the dihedral twists (C , NA , and NB) increase from a relatively flat structure to a more nonplanar structure, the excitation energy increases, and the dipole moment change decreases (data not shown). The transition moment increases when the outer twists are increased (holding the central twist

fixed) and decreases when the central twist is increased (holding the outer twists fixed). The polarizability change increases as the central twist is increased, but its dependence on the outer twists is not monotonic.

The potential energy for angular coordinates is asymmetric, with the energy rising more rapidly as the structure becomes more planar. This behavior is a result of the repulsion between the hydrogen atoms on the benzene rings. Therefore, we expect that geometries with larger twists than the minimum-energy structure contribute more to the ensemble properties than geometries with smaller twists. Hence, the ensemble excitation energy will be larger and the ensemble dipole moment change will be smaller than those of the minimum-energy structure. Because the polarizability change has a more complex dependence on the torsional angles, the result of the ensemble average is not as predictable.

For the 1500 monomers in the 500-trimer collection, a Boltzmann average of the excited-state properties was obtained using

$$\langle X \rangle = \frac{\sum_j \exp[-(E_j - E_0)/k_B T] X_j}{\sum_j \exp[-(E_j - E_0)/k_B T]} \quad (5)$$

where X refers to a property of the monomer that is calculated from eq 1, j is the j th monomer, and E_j and E_0 refer to the heats of formation for the j th monomer and the minimum-energy structure, respectively.

The ensemble averages and fluctuations ($\sqrt{\langle X^2 \rangle - \langle X \rangle^2}$) of the 1500 monomers are $\langle E^m \rangle = 3.76 \pm 0.10$ eV, $\langle |\Delta\mu^m| \rangle = 4.0 \pm 0.7$ D, and $\langle \Delta\alpha^m \rangle = 200 \pm 130$ Å³. These results confirm the above prediction that the monomer ensemble has a higher excitation energy and lower dipole moment change than the minimum-energy structure.

We now compare the ensemble results with the experiments.¹⁷ The ensemble excitation energy is 0.06 eV higher than the experimental absorption maximum, the dipole moment change is about 2 D smaller than the experimental value, and the polarizability change is about twice as large as the experimental value. The inclusion of a weak dielectric environment^{23,24} lowers the excitation energy and the polarizability change and increases the dipole moment change, which helps reconcile the above differences. However, because our primary goal is to study the properties of the trimer in relation to those of the monomer, we focus instead on the property ratios between the trimer and the monomer. Comparisons of these ratios with and without the inclusion of dielectric screening indicate that the ratios are insensitive to dielectric effects (data not shown). Therefore, only gas-phase calculations are reported below.

The depolarization of the fluorescence emission on the blue side of the absorption band of the monomer can be attributed to states that lie above the dominant one-photon state (λ_{\max}) and within the spectral line width. These states carry nonnegligible transition intensity and are polarized at $\sim 90^\circ$ from the dominant state for a monomer that maintains a local C_3 symmetry around the nitrogen atom. Once the monomer is symmetry-broken, these states are polarized at $\sim 120^\circ$, as expected for excitations localized on each benzene ring connected to the nitrogen atom. (Similar polarization effects are seen in the trimer, as in section 3.2.2.) Excitations to these states will be followed by rapid relaxation to the lowest excited state, causing a loss in polarization.

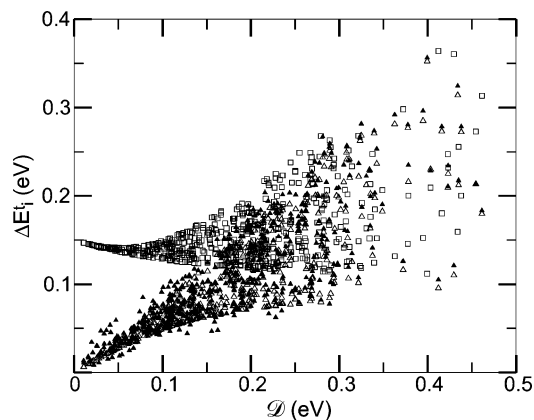


Figure 2. Energy separation ΔE_i^t ($i = 1, 2$) for the 500-trimer collection using both the four-state exciton model (open symbols) and the INDO/SCI method (filled symbols). ΔE_1^t is represented as triangles, and ΔE_2^t as squares. The X coordinate is the energy disorder \mathcal{D} among the three arms.

3.2. Trimer. This section compares the results obtained from the INDO/SCI method, the four-state exciton model, and the diagonal disorder exciton model. In all Figures, open symbols correspond to the four-state exciton model, filled symbols correspond to the INDO/SCI method, and lines correspond to the diagonal disorder exciton model.

3.2.1. Excited-State Energies. The excited states of the trimer are denoted E_i^t ($i = 1, 2, 3$). The energy separations between adjacent states are denoted $\Delta E_1^t = E_2^t - E_1^t$ and $\Delta E_2^t = E_3^t - E_2^t$.

It is useful to introduce a single variable \mathcal{D} that quantifies the energetic disorder among the three arms and the degree of symmetry breaking in the trimer. If the excitation energies of the three arms, E_i^m ($i = 1, 2, 3$), are in ascending order, then \mathcal{D} is defined as $(E_3^m - E_2^m) + (E_2^m - E_1^m) = E_3^m - E_1^m$, which is twice the average energy gap of the monomers (the two gaps being $E_2^m - E_1^m$ and $E_3^m - E_2^m$). When \mathcal{D} is zero, all three monomers share the same excitation energy, E^m , and the trimer is energetically symmetric. The diagonalization of eq 2 produces two degenerate excited states (E symmetry) with energy $E^m - J$ and a third state (A symmetry) with energy $E^m + 2J$. Because $J > 0$, the E states lie below the A state. The four-state exciton model, therefore, predicts that ΔE_1^t is zero and ΔE_2^t is $3J$ at zero disorder. These results are illustrated in Figure 2 at $\mathcal{D} = 0$, which shows ΔE_1^t (triangles) and ΔE_2^t (squares) for the 500-trimer collection using both the four-state exciton model and the INDO/SCI method. (ΔE_2^t results using the INDO/SCI method are not shown in the Figure; see below for analysis.)

In Figure 2, as \mathcal{D} increases, a broad distribution of ΔE_i^t for each \mathcal{D} is observed. This spread arises from plotting multidimensional data against a single variable. To reduce the properties to one dimension (\mathcal{D}), the 500 ΔE_i^t ($i = 1$ or 2) values are grouped into 20 bins according to \mathcal{D} , with each bin 0.025 eV in width. The values collected in each bin are then averaged. We refer to this procedure as the binning-and-averaging approach. The results are plotted in Figure 3.

The binning-and-averaging results (Figure 3) show that as \mathcal{D} increases the degeneracy of the two E states is lifted. ΔE_1^t increases proportionally to \mathcal{D} with a slope of $\sim 1/2$. ΔE_2^t decreases for small \mathcal{D} and then increases and converges toward ΔE_1^t at large \mathcal{D} . At an energetic disorder of about 0.2 eV, ΔE_2^t becomes similar to ΔE_1^t . From this point on, the excitation energies E_i^t ($i = 1, 2, 3$) of the trimer become similar in value

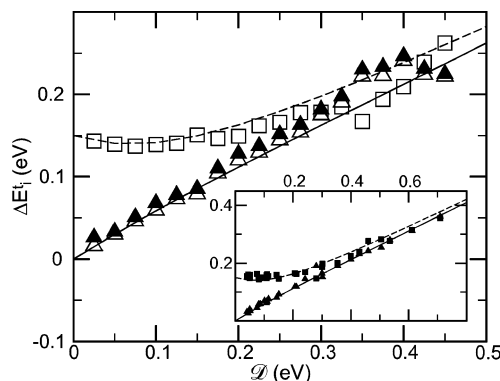


Figure 3. Energy separation ΔE_i^t ($i = 1, 2$) for the 500-trimer collection using both the four-state exciton model (open symbols) and the INDO/SCI method (filled symbols). The inset shows the INDO/SCI results for the 30-trimer collection. ΔE_1^t is represented as triangles, and ΔE_2^t , as squares. The solid line (ΔE_1^t) and the dashed line (ΔE_2^t) are from the diagonal disorder exciton model.

to those of the constituent monomers, E_i^m . We consider $\mathcal{D} = 0.2$ eV to be the cutoff value beyond which the trimer excited states become localized and the trimer structure is completely symmetry-broken.

From Figures 2 and 3, we can see that the correlation of ΔE_1^t between the INDO/SCI results and the four-state exciton model results is excellent. The relative errors between these two approaches are about 0.2% for E_1^t and E_2^t and about 16% for ΔE_1^t (caused by small energy separations). This agreement indicates that using a single value for J in eq 2 is a good approximation. Hence, the effects of off-diagonal disorder are negligible.

The lines in Figure 3 represent the predictions of the diagonal disorder model using the binning-and-averaging procedure on 20 million different matrices of eq 4. The agreement between the diagonal disorder exciton model and the 500-trimer collection results supports the above conclusion that off-diagonal disorder is not important.

ΔE_2^t from the INDO/SCI method for the 500-trimer collection is not shown in Figures 2 and 3 because of difficulty in identifying the relevant third excited state. The first two excited states have large transition moments and hence are easy to distinguish. However, the third state is difficult to identify for many disordered structures because of the existence of many other states close in energy and transition intensity. In the 30-trimer collection (section 2.1), it is possible to identify the third state reliably. In these molecules, the excited states that arise from the mixing of the monomer excitation can be identified on the basis of the following characteristics. First, all three excited states have similar values of charge-transfer character between the molecular segments, independent of \mathcal{D} . Second, at small \mathcal{D} , the three trimer excited states are highly delocalized between the branch segments. Third, as \mathcal{D} increases, the three excited states become increasingly localized on each branch segment, with the lowest-energy state localized on the segment with the lowest E^m and the highest-energy state localized on the segment with the highest E^m .

ΔE_i^t ($i = 1, 2$) of the 30-trimer collection is shown in the inset of Figure 3. In these trimers, because $E_3^m - E_2^m$ and $E_2^m - E_1^m$ are similar in value, \mathcal{D} completely specifies the excited-state energies of the trimer, and no binning-and-averaging is necessary. The results agree with those in the main plot. When \mathcal{D} is zero, the INDO/SCI results predict that ΔE_1^t is zero and ΔE_2^t is ~ 0.15 eV. As shown earlier, ΔE_2^t is predicted to be $3J$

by the four-state exciton model, thus J is 0.05 eV. This assignment is consistent with the least-squares analysis of J in the four-state exciton model (section 2.3).

3.2.2. Excited-State Transition Moments. When the trimer is C_3 -symmetric, the dipole operator in the trimer basis (section 2.3) is

$$\underline{\underline{\mu}}^t - \langle \text{gs} | \underline{\underline{\mu}}^t | \text{gs} \rangle = \begin{pmatrix} \begin{pmatrix} 0 \\ 0 \\ 0 \end{pmatrix} \begin{pmatrix} \sqrt{\frac{3}{2}} TM_y \\ -\sqrt{\frac{3}{2}} TM_x \\ 0 \end{pmatrix} \begin{pmatrix} \sqrt{\frac{3}{2}} TM_x \\ \sqrt{\frac{3}{2}} TM_y \\ \sqrt{3} TM_z \end{pmatrix} \begin{pmatrix} 0 \\ 0 \\ 0 \end{pmatrix} \\ \begin{pmatrix} \sqrt{\frac{3}{2}} TM_y \\ -\sqrt{\frac{3}{2}} TM_x \\ 0 \end{pmatrix} \begin{pmatrix} -\frac{1}{2} \mu_x \\ -\frac{1}{2} \mu_y \\ \mu_z \end{pmatrix} \begin{pmatrix} -\frac{1}{2} \mu_y \\ \frac{1}{2} \mu_x \\ 0 \end{pmatrix} \begin{pmatrix} \frac{1}{\sqrt{2}} \mu_y \\ -\frac{1}{\sqrt{2}} \mu_x \\ 0 \end{pmatrix} \\ \begin{pmatrix} \sqrt{\frac{3}{2}} TM_x \\ \sqrt{\frac{3}{2}} TM_y \\ 0 \end{pmatrix} \begin{pmatrix} -\frac{1}{2} \mu_x \\ \frac{1}{2} \mu_x \\ 0 \end{pmatrix} \begin{pmatrix} \frac{1}{2} \mu_x \\ \frac{1}{2} \mu_y \\ \mu_z \end{pmatrix} \begin{pmatrix} \frac{1}{\sqrt{2}} \mu_x \\ \frac{1}{\sqrt{2}} \mu_y \\ 0 \end{pmatrix} \\ \begin{pmatrix} 0 \\ 0 \\ \sqrt{3} TM_z \end{pmatrix} \begin{pmatrix} \frac{1}{\sqrt{2}} \mu_y \\ -\frac{1}{\sqrt{2}} \mu_x \\ 0 \end{pmatrix} \begin{pmatrix} \frac{1}{\sqrt{2}} \mu_x \\ \frac{1}{\sqrt{2}} \mu_y \\ \mu_z \end{pmatrix} \begin{pmatrix} 0 \\ 0 \\ \mu_z \end{pmatrix} \end{pmatrix} \quad (6)$$

We introduce the following notations for $\underline{\underline{\Delta\mu}}^m$ and $\underline{\underline{TM}}^m$ of the monomer:

$$\underline{\underline{\Delta\mu}}^m = \begin{pmatrix} \mu_x \\ \mu_y \\ \mu_z \end{pmatrix} \quad (7)$$

and

$$\underline{\underline{TM}}^m = \begin{pmatrix} TM_x \\ TM_y \\ TM_z \end{pmatrix} \quad (8)$$

The trimer basis of eq 6 is ordered as the ground state, the two E states, and the A state. Equation 6 is in agreement with the results of Beljonne et al.⁷ obtained using a similar model.

Because the monomer's transition moment from the ground state to the dominant excited state lies in the X - Y plane ($TM_z = 0$ in eq 8), the A state of a C_3 -symmetric trimer is predicted to be dark. The E states are predicted to have perpendicular transition moments with equal magnitudes such that the total optical intensity is 3 times that of the monomer. These predictions are confirmed by INDO/SCI calculations on a series of trimer structures with C_3 symmetry (data not shown).

Figure 4 shows the results of applying the binning-and-averaging procedure discussed in section 3.2.1 to the transition moments, $|TM_i^t|$ ($i = 1, 2, 3$), of the 500-trimer collection (main plot) and the 30-trimer collection (inset). As \mathcal{D} increases and the C_3 symmetry of the trimer is broken, the A state quickly gains optical intensity whereas the two E states lose intensity and become nonequivalent. At large \mathcal{D} , the transition moments of all three states converge toward the monomer value of about 7 D (section 2.4).

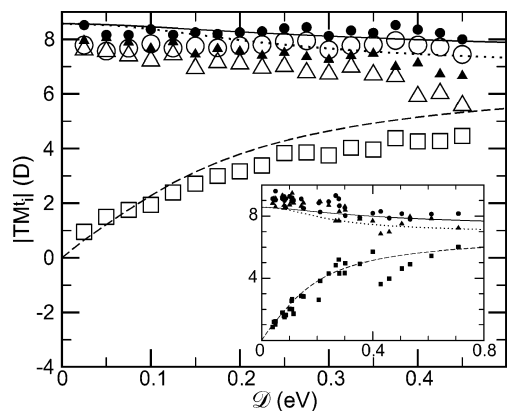


Figure 4. Transition moment $|TM_i^t|$ for the 500-trimer collection ($i = 1, 2, 3$ for the four-state exciton model and $i = 1, 2$ for the INDO/SCI method). The inset shows the INDO/SCI 30-trimer collection results for all three states. $|TM_1^t|$ is represented as circles or solid lines, $|TM_2^t|$ is represented as triangles or dotted lines, and $|TM_3^t|$ is represented as squares or dashed lines. The convention for symbols and lines is the same as in Figure 3.

Excellent agreement between the four-state exciton model and the INDO/SCI method is illustrated in Figure 4, indicating that the use of $J = 0.05$ eV in eq 2 is a good approximation and the effects of off-diagonal disorder are minimal. There is, however, a slight disagreement between the results of the 500-trimer collection and the predictions of the diagonal disorder exciton model. This is attributed to dipole-operator disorder that is included in the collection studies but ignored in the diagonal disorder exciton model.

As \mathcal{D} increases, the angle between \underline{TM}_1^t and \underline{TM}_2^t changes from 90° toward 120° . These angles are expected for systems with C_3 symmetry and for systems with complete symmetry breaking, respectively (data not shown). These angle changes provide another measure of the degree of symmetry breaking in the trimer.

3.2.3. Excited-State Dipole Moment Changes. We next consider the measured change in dipole moment. A change in dipole moment causes the electroabsorption spectrum to have a component that is proportional to the second derivative of the absorption spectrum. For a centrosymmetric molecule, the appearance of this second derivative in the electroabsorption spectrum is a clear indication of symmetry breaking. For C_3 -symmetric molecules, the presence of E symmetry states makes the situation less straightforward. Hochstrasser²⁶ used group theory to show that E symmetry states can exhibit a first-order Stark effect and thus should exhibit a second derivative signal in electroabsorption. Talanina et al.²⁷ verified this by extending the Liptay formulation of electroabsorption²⁸ to D_3 -symmetric molecules. Here, we extend this analysis to consider how the second derivative component of the electroabsorption spectrum should vary between the monomer and the trimer, under various assumptions regarding the degree of symmetry breaking in the trimer.

The prediction of the electroabsorption spectrum is complicated by the nature of the dipole operator in eq 6. The two degenerate E states have dipole moments that are equal in magnitude but opposite in direction. In addition, the dipole operator has matrix elements between the two degenerate E states such that the eigenstates of the Hamiltonian in an electric field depend on the orientation of the applied field. In the Supporting Information of this paper, we extend Ponder's formalism²⁹ for electroabsorption to molecules with degenerate

TABLE 3: Dipole Moment Change of the Trimer $\Delta\mu^t$ for Different Ranges of Disorder^a

	zero disorder	intermediate disorder	large disorder
\mathcal{D} (eV)	<0.016	$0.016\ldots0.20$	>0.20
$\Delta\mu^t$	$1/\sqrt{2}\mu^m$	$1/2\mu^m$	μ^m
excited state	delocalized	delocalized	localized

^a μ^m indicates the dipole moment change of the monomer. \mathcal{D} is the energetic disorder defined in section 3.2.1.

excited states of E symmetry, taking full account of the complexities resulting from the dipole operator of eq 6. The derivation includes an average over all orientations of the molecule, assuming an isotropic sample. We set the angle between the applied field and the polarization of the light at the magic angle (54.7°), as in the experimental measurements. By comparing the second-derivative spectrum predicted for a nondegenerate excited state (the monomer) with that expected for a degenerate excited state (the symmetric trimer), we can obtain the expected ratio of the change in dipole moment measured for the trimer to that for the monomer. We consider three different assumptions regarding the degree of symmetry breaking, which are summarized in Table 3 and discussed in turn below.

For a symmetric trimer, the ratio between the dipole moment change extracted from an electroabsorption spectrum of the trimer and that of a monomer should be $1/\sqrt{2}$. At the other extreme, when the disorder is sufficient to break the symmetry completely, the dipole moment change of the monomer and trimer should be identical, corresponding to a ratio of 1. This occurs when \mathcal{D} is greater than $4J$ or 0.2 eV. We can also envision an intermediate degree of disorder, which is small compared to $4J$ but large compared to the dipole coupling between the E states. For the trimer structure studied here, this dipole coupling is quite small. The largest field applied in the experiments is 10^6 V·cm⁻¹,¹⁷ leading to a dipole coupling energy of ~ 0.004 eV (using the average dipole moment change of 4 D obtained from the 1500 monomer collection). This yields an energy splitting between the two E states of 0.008 eV. When \mathcal{D} is greater than twice this splitting, 0.016 eV,³⁰ but much less than $4J$, the excited states of the trimer remain delocalized, but the degeneracy of the E states has been lifted to an extent such that the dipole coupling between them can be ignored. Under these assumptions for intermediate disorder, the ratio between the dipole moment change of the trimer and the monomer is predicted to be $1/2$.

For the structures in both the 500- and 30-trimer collections, the energetic disorder among the arms falls under the intermediate or large disorder categories. For the 500-trimer collection (Figure 2), the smallest energy separation between the two E states is greater than 0.01 eV, which is larger than the 0.008 eV dipole splitting. For the 30-trimer collection, the smallest E-state energy separation is greater than 0.02 eV, which is also larger than 0.008 eV. Because the dipole coupling between the E states can be ignored, the intensity-weighted average of eq 1 can be used for all of the trimers in the collections.

The results obtained for the two trimer collections are summarized in Figure 5. The binning-and-averaging procedure discussed in section 3.2.1 is applied to the transition intensity-weighted dipole moment change, $\Delta\mu^t$, obtained from eq 1. As \mathcal{D} increases and the C_3 symmetry of the trimer is broken, $\Delta\mu^t$ increases from one-half the monomer value at $\mathcal{D} = 0$ to nearly the monomer value at large \mathcal{D} , as expected. We note that at zero disorder the trimer dipole moment change obtained from the diagonal disorder exciton model (lines in Figure 5) is one-half the value of the monomer dipole moment change. This is

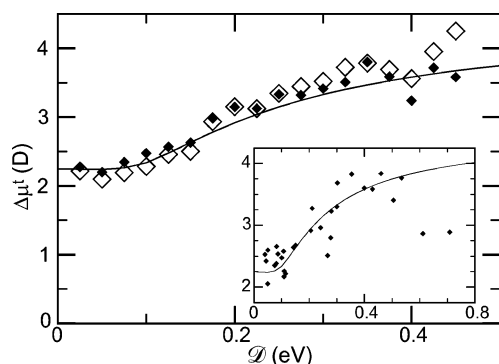


Figure 5. Transition intensity-weighted dipole moment change $\Delta\mu^\dagger$ from eq 1 for the 500-trimer collection. For the INDO/SCI results (filled symbols), all three excited states (two E states and one A state) are included in the 30-trimer collection (inset), and only the first two excited states (two E states) are included in the 500-trimer collection (main plot). The symbol and line convention is the same as in Figure 3.

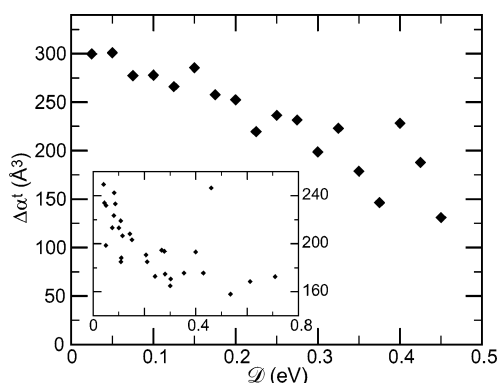


Figure 6. Transition intensity-weighted polarizability change $\Delta\alpha^\dagger$. The INDO/SCI method was used for both collections. All three excited states (two E states and one A state) are included in the 30-trimer collection (inset), and only the first two excited states (two E states) are included in the 500-trimer collection (main plot).

because the diagonal disorder exciton model studies the trimer in the absence of an external electric field and considers only the expectation value of the dipole operator to derive the dipole moment change, thus the dipole coupling between the E states is not included in the model.

Similar to the energy and transition moment, excellent agreement is obtained between the INDO/SCI method and the four-state exciton model for the 500-trimer collection. The relative error between these two methods is $\sim 10\%$. However, small differences are observed between the 500-trimer collection and the diagonal disorder exciton model. These are attributed to disorder in the dipole operator, as was also seen for the transition moment (section 3.2.2).

3.2.4. Excited-State Polarizability Changes. The exciton models of section 2.3 and 2.4 make it possible to express the energies, the transition moments, and the dipole moment changes of the trimer in terms of those of the monomer. To connect the polarizability changes of the trimer to those of the monomer, more complicated models are required, such as those that consider higher excited states. These models are not studied in this work. Because the exciton models do not consider the polarizability changes of the monomer and the trimer, we will discuss only the INDO/SCI results here.

Figure 6 shows the results of applying the binning-and-averaging procedure of section 3.2.1 to the transition intensity-weighted polarizability change. Equation 1 is used because these structures contain disorder in the intermediate or large disorder regimes (section 3.2.3). In the Figure, as the C_3 symmetry of

the trimer is broken, $\Delta\alpha^\dagger$ decreases toward the monomer's polarizability change. The average $\Delta\alpha^\dagger$ (and fluctuations $\sqrt{\langle X^2 \rangle - \langle X \rangle^2}$) over the 500 trimers is $250 \pm 100 \text{ \AA}^3$, which is close to the monomer ensemble average of $200 \pm 130 \text{ \AA}^3$.

4. Discussion and Summary

This article examines the photophysics of a model dendrimer using simple exciton models to relate the properties of the dendrimer to its constituent subunits. In addition, INDO/SCI calculations are used to connect structural disorder to energetic disorder and study the resulting disorder-induced symmetry breaking.

The four-state exciton model uses the excited-state properties of the monomer obtained from the INDO/SCI calculations to predict the properties of the trimer, assuming the coupling between the arms, J , is a constant. Excellent agreement is found between this model and explicit INDO/SCI calculations on the trimer for the excited-state properties, including the energy, transition moment, and dipole moment change. This agreement supports the assumption of a constant coupling, J , and indicates that the effects of off-diagonal disorder are not significant in these systems. The comparisons of the diagonal disorder exciton model with the four-state exciton model and the INDO/SCI method confirm that diagonal disorder plays a dominant role in the symmetry breaking. In the exciton models, the interbranch coupling energy J is found to be 0.05 eV ($\sim 400 \text{ cm}^{-1}$) from a least-squares analysis of the excited-state energies and dipole moment changes, in agreement with the prediction of INDO/SCI calculations (section 3.2.1). This J value is similar to the 0.033 eV found in analogous dendrimers.⁷

The effects of symmetry breaking can be studied by introducing a single variable \mathcal{D} that describes the energetic disorder among the arms. \mathcal{D} is the total spread in excitation energy between the arms, $E_3^m - E_1^m$. The binning-and-averaging procedure of section 3.2.1 effectively reduces the system to one dimension so that the photophysical properties of the trimer can be studied as functions of the disorder, \mathcal{D} . Figures 3–6 reveal the following trends. When the disorder of the trimer is small, the relevant excited states are highly delocalized, with two degenerate bright E states red-shifted by J and a dark A state blue-shifted by $2J$ from the monomer. The dipole moment change of the trimer is about half that of the monomer, and the polarizability change is nearly twice that of the monomer. When the disorder of the trimer is large ($\mathcal{D} > 4J$), the trimer behaves like three individual monomers. The trimer excited states are localized with excitation energies similar to those of the constituent monomers. All three states now carry optical intensity that is similar to that of the monomers, and both the dipole moment change and the polarizability change of the trimer approach those of the constituent monomers.

The above trends, in comparison with the electroabsorption measurements,¹⁷ suggest that the trimer sample is symmetry-broken because the experimental dipole moment change of the trimer is similar to that of the monomer and the experimental polarizability change of the trimer is only slightly larger than that of the monomer. The dipole moment change is the most sensitive to symmetry breaking (Figure 5) and provides the strongest evidence for symmetry breaking in the trimer. In the Supporting Information, we show that the appearance of a second derivative electroabsorption signal is not a sufficient argument for symmetry breaking in the structure. Instead, it is the relative magnitude of the dipole moment change of the trimer and its constituent arm that is the clearest evidence of symmetry breaking. This dipole moment change ratio is $1/\sqrt{2}$ for com-

pletely symmetric trimers, $1/2$ for trimers with intermediate disorder, and 1 for symmetry-broken trimers.

Figures 3–6 show that the symmetry of the trimer is broken when the energetic disorder, \mathcal{D} , is greater than 0.2 eV (4*J*). We can use this to infer the distribution of monomer excitation energies that is needed to break symmetry. If this distribution is Gaussian with a standard deviation of 0.14 eV, then the difference in energy between the two arms that define \mathcal{D} would have a standard deviation of $\sqrt{2} \times 0.14$ eV, corresponding to the 0.2 eV required for symmetry breaking.³¹ Trimers made with arms more varied than 0.14 eV would be completely symmetry-broken. In section 3.1, the ensemble average of the monomer excitation energy from the 500-trimer collection has a standard deviation of 0.10 eV at room temperature, which is slightly smaller than the above estimate of 0.14 eV required for complete symmetry breaking in the trimer. Therefore, the disorder required for symmetry breaking in the trimer is larger than the disorder found in a room-temperature thermal distribution.

Because the inhomogeneous line width (fwhm) is 2.355 times the standard deviation of the excitation, a line width of greater than $2.355 \times 0.14 = 0.33$ eV for the arms should be sufficient to lead to symmetry breaking. The experimental line width for the trimer sample is 0.4–0.5 eV. This is greater than 0.33 eV and so is consistent with the sample being symmetry-broken. Furthermore, at large disorder, the absorption of the trimer should become equivalent to that of the monomer. However, the line width of the trimer sample is about 0.1 eV smaller than that of the monomer sample. This suggests that the arms are more ordered in the trimer than in the monomer.

Two additional pieces of evidence suggest that the monomer sample used in the experiment is more disordered than the trimer sample. The first piece of evidence is based on the spectral shift of the absorption from the monomer to the trimer. This shift is predicted to be *J* for an ordered system and to decrease toward zero as symmetry is broken. The experimental red shift of 0.16 eV can be rationalized in terms of the arms being more disordered (larger dihedral twists, higher excitation energies) in the experimental monomer samples than in the trimer samples. The second piece of evidence is based on the observed dipole moment changes. The predicted change in the dipole is $1/\sqrt{2}$ that of the monomer for a symmetric dendrimer, one-half that of the monomer for a nearly-ordered system, and equal to that of the monomer for a disordered system (Figure 5). However, experiments find the dipole moment change of the trimer (6.9 D) to be slightly larger than that measured for the monomer samples (6.0 D). Disorder lowers the dipole moment change of the monomer; therefore, this observation also suggests that the arms are more disordered in the monomer samples than in the trimer samples.

INDO/SCI calculations allow us to connect structural disorder to energetic disorder. Calculations on monomers with various dihedral twists (C, NA, and NB) indicate that the effects of geometric distortions are approximately additive. A 5° increase in any one of the dihedral twists causes an increase of ~0.02 eV in the excitation energy of the monomer (data not shown). If all three dihedral twists (C, NA, and NB) contribute equally to the inhomogeneous line width, then a standard deviation of 0.14 eV/ $\sqrt{3}$ or 0.08 eV in each angle is needed. This corresponds to a ~20° average deviation of each dihedral angle from its optimal value. Thus, the observed symmetry breaking can be attributed to structural disorder of greater than 20° in the dihedral angles.

In summary, we constructed two exciton models of a dendrimer and tested them by comparison to INDO/SCI

calculations on a collection of disordered structures. The results verify the use of exciton models on such systems and indicate that off-diagonal disorder and dipole-operator disorder do not play significant roles in the symmetry breaking. A binning-and-averaging procedure was developed that allows the properties to be studied as a function of a single variable, \mathcal{D} , that defines the energetic disorder of the system. For the dendrimer considered here, energetic disorder of greater than 4*J* or 0.2 eV is needed to account for the experimentally observed symmetry breaking. This is larger than the energetic disorder predicted for structures present in a room-temperature thermal distribution, which indicates that the disorder in the glassy experimental samples is larger than thermal. This work also emphasizes that the relative magnitude of the dipole moment change between the dendrimer and its branches is indicative of the degree of symmetry breaking in the dendrimer structure.

Acknowledgment. L.A.L. was supported by a Graduate Fellowship from the Merck Computational Biology and Chemistry Program at Carnegie Mellon University established by the Merck Company Foundation. D.J.Y. thanks the NSF (grant no. 0316759) for funding.

Supporting Information Available: Detailed derivation of the electroabsorption spectrum for isotropic C₃-symmetric molecules, including the results in Table 3. This material is available free of charge via the Internet at <http://pubs.acs.org>.

References and Notes

- (1) Zyss, J.; Ledoux, I. *Chem. Rev.* **1994**, *94*, 77.
- (2) Cho, B. R.; Son, K. H.; Lee, S. H.; Song, Y.-S.; Lee, Y.-K.; Jeon, S.-J.; Choi, J. H.; Lee, H.; Cho, M. *J. Am. Chem. Soc.* **2001**, *123*, 10039.
- (3) Kopelman, R.; Shortreed, M.; Shi, Z.-Y.; Tan, W.; Xu, Z.; Moore, J. S.; Bar-Haim, A.; Klafter, J. *Phys. Rev. Lett.* **1997**, *78*, 1239.
- (4) Meskers, S. C. J.; Bender, M.; Hübner, J.; Romanovskii, Y. V.; Oestreich, M.; Schenning, A. P. H. J.; Meijer, E. W.; Bässler, H. *J. Phys. Chem. A* **2001**, *105*, 10220.
- (5) Tretiak, S.; Chernyak, V.; Mukamel, S. *J. Phys. Chem. B* **1998**, *102*, 3310.
- (6) Poliakov, E. Y.; Chernyak, V.; Tretiak, S.; Mukamel, S. *J. Chem. Phys.* **1999**, *110*, 8161.
- (7) Beljonne, D.; Wenseleers, W.; Zojer, E.; Shuai, Z.; Vogel, H.; Pond, S. J. K.; Perry, J. W.; Marder, S. R.; Brédas, J.-L. *Adv. Funct. Mater.* **2002**, *12*, 631.
- (8) Lee, W.-H.; Lee, H.; Kim, J.-A.; Choi, J.-H.; Cho, M.; Jeon, S.-J.; Cho, B. R. *J. Am. Chem. Soc.* **2001**, *123*, 10658.
- (9) Lupton, J. M.; Samuel, I. D. W.; Burn, P. L.; Mukamel, S. *J. Phys. Chem. B* **2002**, *106*, 7647.
- (10) Jiang, D.-L.; Aida, T. *Nature* **1997**, *388*, 454.
- (11) Nomura, Y.; Sugishita, T.; Narita, S.; Shibuya, T. *Bull. Chem. Soc. Jpn.* **2002**, *75*, 481.
- (12) Harigaya, K. *Phys. Chem. Chem. Phys.* **1999**, *1*, 1687.
- (13) Verbouwe, W.; Viaene, L.; Van der Auweraer, M.; De Schryver, F. C.; Masuhara, H.; Pansu, R.; Faure, J. *J. Phys. Chem. A* **1997**, *101*, 8157.
- (14) Verbouwe, W.; Van der Auweraer, M.; De Schryver, F. C.; Piet, J. J.; Warman, J. M. *J. Am. Chem. Soc.* **1998**, *120*, 1319.
- (15) Schuddeboom, W.; Warman, J. M.; Van der Auweraer, M.; De Schryver, F. C.; Declercq, D. D. *Chem. Phys. Lett.* **1994**, *222*, 586.
- (16) Verbeek, G.; Depaemelaere, S.; Van der Auweraer, M.; De Schryver, F. C.; Vaes, A.; Terrell, D.; De Meutter, S. *Chem. Phys.* **1993**, *176*, 195.
- (17) Bangal, P. R.; Lam, D. M. K.; Peteanu, L. A.; Van der Auweraer, M. *J. Phys. Chem. B* **2004**, *108*, 16834.
- (18) Martín-Delgado, M. A.; Rodríguez-Laguna, J.; Sierra, G. *Phys. Rev. B* **2002**, *65*, 155116.
- (19) Dewar, M. J. S.; Zoebisch, E. G.; Healy, E. F.; Stewart, J. J. P. *J. Am. Chem. Soc.* **1985**, *107*, 3902.
- (20) Trial calculations on a 1,3,5-triarylbenzene yielded a minimum geometry with a central twist of ~45° using the AM1 Hamiltonian, which agrees with spectroscopic measurements by Bastiansen, O. *Acta Chem. Scand.* **1952**, *6*, 205. On the contrary, a planar structure was found to be the minimum using the PM3 Hamiltonian.
- (21) When NA and NB share the same sign, the three benzene rings connected to the nitrogen in the monomer are arranged in a fashion that is analogous to a propeller. When NA and NB are of oppo-

site signs, the two outer rings are positioned with respect to the middle ring in a fashion that is analogous to a butterfly. The butterfly-type monomers have much higher ($>3k_B T$) heats of formation than those of the propeller type and hence are not included in the 1500-monomer collection.

- (22) Tomlinson, A.; Yaron, D. *J. Comput. Chem.* **2003**, *24*, 1782.
- (23) Wachsmann-Hogiu, S.; Peteanu, L. A.; Liu, L. A.; Yaron, D. J.; Wildeman, J. *J. Phys. Chem. B* **2003**, *107*, 5133.
- (24) Chowdhury, A.; Yu, L.; Raheem, I.; Peteanu, L.; Liu, L. A.; Yaron, D. J. *J. Phys. Chem. A* **2003**, *107*, 3351.
- (25) Pasquinelli, M. A. An Effective Particle Approach to the Photo-physics of Conjugated Polymers. Ph.D. Thesis, Carnegie Mellon University, 2002.
- (26) Hochstrasser, R. M. *Acc. Chem. Res.* **1973**, *6*, 263.
- (27) Talanina, I. B.; Collins, M. A.; Dubicki, L.; Krausz, E. *Chem. Phys. Lett.* **1992**, *200*, 318.
- (28) Liptay, W. In *Excited States*; Lim, E. C., Ed.; Academic Press: New York, 1974; Vol. 1, p 161.
- (29) Ponder, M. C. Electric Field Spectroscopy of Diphenylpolyenes, All-trans Retinal, and Bacteriorhodopsin. Ph.D. Thesis, University of California, Berkeley, California, 1983.
- (30) The energy separation between the two E states is about one-half that of the energetic disorder \mathcal{D} , as illustrated in section 3.2.1.
- (31) If x and y are random variables with a Gaussian distribution that has a standard deviation of σ , then the addition or subtraction of these two variables $x \pm y$ has a Gaussian distribution with a standard deviation of $\sqrt{2}\sigma$. This is analogous to error propagation (Harris, D. C. *Quantitative Chemical Analysis*, 3rd ed.; Freeman: New York, 1991).